Human-Robot Co-Navigation using Anticipatory Indicators of Human Walking Motion

Vaibhav V. Unhelkar*[1], Claudia Pérez-D'Arpino*[1], Leia Stirling[2] and Julie A. Shah[1]

***Abstract*— Mobile, interactive robots that operate in human-centric environments need the capability to safely and efficiently navigate around humans. This requires the ability to sense and predict human motion trajectories and to plan around them. In this paper, we present a study that supports the existence of statistically significant biomechanical turn indicators of human walking motions. Further, we demonstrate the effectiveness of these turn indicators as features in the prediction of human motion trajectories. Human motion capture data is collected with predefined goals to train and test a prediction algorithm. Use of anticipatory features results in improved performance of the prediction algorithm. Lastly, we demonstrate the closed-loop performance of the prediction algorithm using an existing algorithm for motion planning within dynamic environments. The anticipatory indicators of human walking motion can be used with different prediction and/or planning algorithms for robotics; the chosen planning and prediction algorithm demonstrates one such implementation for human-robot co-navigation.**

I. INTRODUCTION

Various applications within service and industrial domains often require mobile robots capable of operating within proximity to humans. Safe and autonomous navigation in human-centric environments is an important prerequisite for such interactive robots. Autonomous path/motion planning is a classic problem in robotics [1]. Although multiple successful motion planning algorithms have been developed that have enabled the current navigation capabilities of modern robots, online motion planning within dynamic, uncertain environments is still an active area of research [2]. Robots that operate in human-centric environments require co-navigation, i.e., a system that can reason and plan around humans and other dynamic obstacles online, efficiently and in a human-intuitive fashion.

The challenge of robot navigation while in proximity to humans includes aspects of physical human-robot interaction, wherein both robot and human agents must plan and execute trajectories toward goal locations that may interact with the trajectories of other agents in the environment. Robots that are deployed to assist and function alongside humans must ensure that the interaction between these trajectories is safe, fluent and nonintrusive from the humans' perspective. Ideally, a mobile robot should minimize disruptions to human trajectories toward a goal location.

A reliable human motion prediction capability can lead to improved decision-making. For instance, in day-to-day interactions, humans often predict the intention and motion of other agents within their environment in order to plan, schedule and execute tasks. Similarly, prior studies of human-robot collaboration have indicated that social robots that can anticipate human intention are capable of more fluent interaction [3]. Thus, we posit that in order to be effective, a robot navigating around humans must be capable of both predicting the motion of dynamic obstacles (including humans) and using this predictive information to plan safe and purposeful paths.

Existing approaches that address the problem of robot path planning in proximity to humans have incorporated both of these aspects at different levels of detail [4]–[8]. Here, we focus on improving human motion prediction through the use of human walking motion features that have been identified as statistically significant in prior biomechanical studies. We posit that these features can augment existing path and motion prediction approaches, resulting in improved path planning performance.

We begin with a brief discussion of the existing methods for robot path planning in proximity to humans. Next, we report the results from a human motion study that extends previously reported anticipatory turn signals [9], [10] to loosely constrained human walking motion. We demonstrate the effectiveness of these signals by incorporating them as features in an algorithm [11] designed to predict human walking motion. Lastly, we evaluate the closed-loop performance of these features by using this prediction algorithm along with an existing path planner for a dynamic environment [12] in simulation.

We wish to emphasize that the features can be used with different prediction and/or planning algorithms while developing a navigation system for mobile, interactive robots. The prediction and planning algorithms presented here demonstrate one such implementation.

II. RELATED WORK

As mentioned in Section I, autonomous path planning while in proximity to humans requires robots to both infer the prospective path of the human agents and reason about this anticipatory (and usually stochastic) information in order to come up with feasible motion plans in real-time. Here, we briefly describe some existing methods of addressing both of these sub-problems, and prior art focused on integrating them to develop path planners for human-robot interaction scenarios.

*These authors contributed equally to this work.

[1]Unhelkar, Pérez-D'Arpino and Shah are with the Computer Science and Artificial Intelligence Laboratory (CSAIL), Massachusetts Institute of Technology unhelkar@mit.edu, cdarpino@mit.edu, julie_a_shah@csail.mit.edu

[2]Stirling is with the Man Vehicle Lab, Department of Aeronautics and Astronautics, Massachusetts Institute of Technology.

A. Path Planning for Robots Working Among Humans

With the advent of social robots and autonomous vehicles, there has been significant interest in developing path-planning approaches for dynamic environments. Though still an active area of research, various algorithms have already been developed and used, such as anytime extensions of classical motion planning algorithms including both grid-based (such as A*) and randomized approaches (such as rapidly exploring random trees [RRT]) [13], [14].

Several methods for the integration of planning and prediction have been considered for developing path-planning systems around humans and other dynamic obstacles. One study [4] uses velocity obstacles to plan around humans. Gaussian processes for prediction and a probabilistic extension of RRT are used to plan paths for dynamic environments in [15]. The generation of safe paths is critical in dynamic and uncertain environments; [16] provides a reachability-based extension of Gaussian processes to better predict human motion, and uses chance-constrained RRT to plan safe paths. In another study [12], researchers developed a grid-based anytime extension of ARA* and demonstrated its effectiveness assuming that predictive information was available regarding dynamic obstacles.

As path-planning in a human-centric environment essentially constitutes a case of human-robot interaction, researchers have assessed navigation not just as a predict-and-plan system, but have also considered interaction and human factors issues [17], [18]. Sisbot et al. [19] presented one of the first approaches to human-aware motion planning. Modeling the human-robot interaction is necessary for indoor environments, where the motion of human agents in the environment will be influenced by that of the robot [20]. Trautman [7] models this *cooperative* navigation using an interaction function, and treats path planning as an inference problem over the joint space. A mixed-observability Markov decision process (MOMDP)-based model is used to reason about the intent and/or goals of human agents and plan around them in [8]. Studies concerning human factors issues include considerations of safety, proxemics and the legibility and predictability of robot motion [21]–[23].

B. Prediction of Human Motion

The modeling and prediction of human motion is of direct interest in multiple domains, including robotics, orthotics, video games and crowd simulation. Initial approaches to predicting human motion included Kalman or particle filtering-based methods, which model the problem of human motion prediction as one of tracking. For service robotics applications, [24] used expectation minimization to learn motion patterns in an environment, and hidden Markov models (HMM) for prediction. Ziebart et al. [5] reported improved results with a predictor that models the intention and decision-making behavior of human motion. More recently, [6] included as features both physical properties of human motion and topological properties, and incorporated prediction of continuous trajectories.

The social forces method [25] and its variants have been utilized for the simulation and prediction of pedestrian motion in crowds. Further, instead of predicting individual motion, [26] used inverse reinforcement learning to learn features of crowd motion and plan around them. Along with the prediction of human motion, researchers have also evaluated the general problem of predicting the motion of dynamic, uncertain objects. Employing Bayesian nonparametric methods to model motion patterns, [27], [28] demonstrated the prediction of the motion of cars through the use of prior GPS data indicating car trajectories.

We believe that, along with the above, the inclusion of biomechanical features of human walking motion may further benefit prediction performance. In the following sections, we evaluate whether anticipatory turn signals of human walking motion can further bolster this predictive capability.

III. ANTICIPATORY INDICATORS OF HUMAN WALKING MOTION

Prior gate studies have demonstrated the existence of anticipatory turn signals in human walking motion across both adult and child populations [9], [10]. Specifically, the indicators velocity of body center of mass, head orientation and foot orientation have been shown to provide anticipatory information regarding human turns in controlled biomechanical studies with pre-specified turn locations. We aimed to observe whether these indicators exist in loosely specified human walking motion - i.e., cases in which humans are free to choose their paths in order to reach goals within the environment.

We performed a human walking study in which only start and goal locations were specified, while the turn location and path were not. Specifically, through a study analyzing human walking motion in a motion capture environment, we evaluated the hypotheses that (a) head orientation (ψ) and (b) body velocity normalized by height ($\bar{v}_x$) can anticipate a turning motion. Analysis of the experimental data indicates evidence of the existence of anticipation via both turn signals.

A. Methods and Protocol

Experiment Protocol: The experiment required participants to walk from a starting location to one of five goals (G-1 through G-5) located within a room, as shown in Fig. 1.

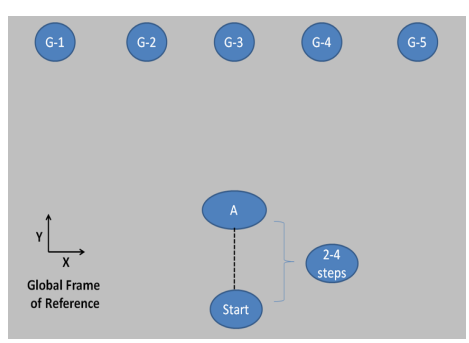

Fig. 1: Overview of the experimental setup. Region A denotes the region after which participants were free to choose their trajectories.

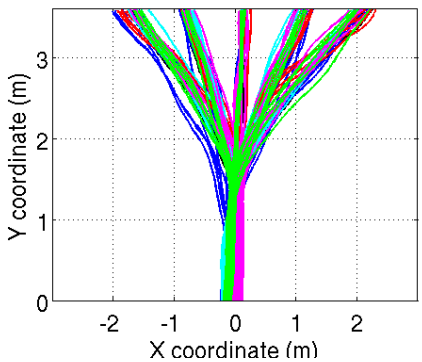

Fig. 2: Trajectories across all the participants: segmented based on the subject (the colors correspond to the trials for different subjects).

Each participant performed 25 such trials, where each goal was assigned five times in a randomized order. The goal location was specified at the start of each run. All runs involved movement along an initial straight-line path until reaching region A (to avoid transient effects due to gait initiation), after which participants were free, and specifically instructed, to choose their own paths to the specified goal locations. Although participants were free to rest between the trials, none exercised this option.

Six participants with a median age of 23.5 years (max: 29, min: 21 years), all of whom were healthy individuals with the ability to walk without assistance, performed the experiment. [1]

Data Collection and Processing: Each participant wore a hard hat, with Vicon markers, and four Vicon plates, each placed at the subject's umbilicus, back, left and right lower feet. The Vicon markers on the hard hat were used to measure head motion, while body motion was approximated by the Vicon object placed at the umbilicus. The data collected via Vicon was exported to Matlab®[2] for processing. To correct for any missing data due to occluded motion capture markers, the obtained motion data was first re-sampled at 100 Hz using Matlab's interpolation function. Next, the data was smoothed using a two-way, 6th-order, Butterworth low pass filter with a cut-off frequency of 10 Hz.

Figure 2 depicts a total of 150 processed trajectories across the goal locations and subjects. The head orientation data was obtained based on the hard hat *object*, and the body position and velocity were obtained from the Vicon *object* placed at the umbilicus. Velocity was calculated using an 8th-order, discrete derivative of the position signal. The algorithm for calculating this derivative was adopted from [29]. The velocity was normalized using the subject's height; as no anthropometric data was collected, height was approximated by averaging the height of the hard hat across all trajectories. For the statistical analysis, the data for head yaw (ψ), body position (x and y coordinate) and body velocity ($\bar{v}_x$) were analyzed at 10 discrete points. These points were obtained through discretization along the y-coordinate at an interval of 0.4m, and averaged across a length span of ± 0.1 m around the discretized point.

[1]The experimental protocol was approved by the Massachusetts Institute of Technology's institutional review board Committee on the Use of Humans as Experimental Subjects (COUHES).

[2]`http://www.mathworks.com/products/new_products/release2012a.html`

B. Data Analysis

The experiment incorporated a repeated measures design with one treatment (a goal location with five levels) and five replicates per condition. The data was analyzed using a two-way, mixed factor ANOVA, with the blocking variable as the subject (random variable) and the treatment as the goal location (fixed variable). The data was analyzed to confirm the residuals were normally distributed. A total of 30 hypotheses, three at each of the 10 discretized y-locations for the dependent variables x, ψ and $\bar{v}_x$, are evaluated. Hence, the set of independent variables included the treatment (goal location), subject and y-location; while the dependent variables included x, ψ and $\bar{v}_x$. The turn signals were considered *anticipatory* if difference existed across goal locations for ψ or $\bar{v}_x$ at an earlier y-location than that for the dependent variable x, which represented the physical turn. The procedure for the statistical analysis for each hypothesis was as follows:

- Fitting the measured data to an ANOVA mixed effects model (1 fixed factor, 1 random factor, and 5 replicates)
- F-tests for main and interaction effects
- Estimation of variances corresponding to random effects
- Tukey's test for pairwise comparison of fixed effects

C. Results

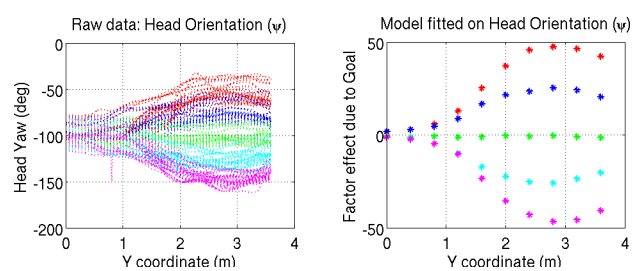

(a) Raw data corresponding to ψ (b) Goal location effects for ψ

Fig. 3: Fitted coefficients of ANOVA, corresponding to the fixed factor, for dependent variable ψ consolidated across all y-locations.

Fitted coefficients of the ANOVA mixed effects model for the fixed effect can be consolidated in one plot across all the y-locations to observe the evolution of the dependent variable along the path. Fig. 3b shows one such plot of the fitted coefficients for the dependent variable ψ across all y-locations, obtained using the raw data presented in Fig. 3a. Since the model accounts for both main and interaction effects, the fitted coefficient α_i includes only the contribution due to the fixed effect (here, the goal location). Also, although the fixed effect is not statistically significant across all y-locations, the coefficients α_i are available across all y-locations and provide a graphical indication of the different values for the dependent variable according to the goal location.

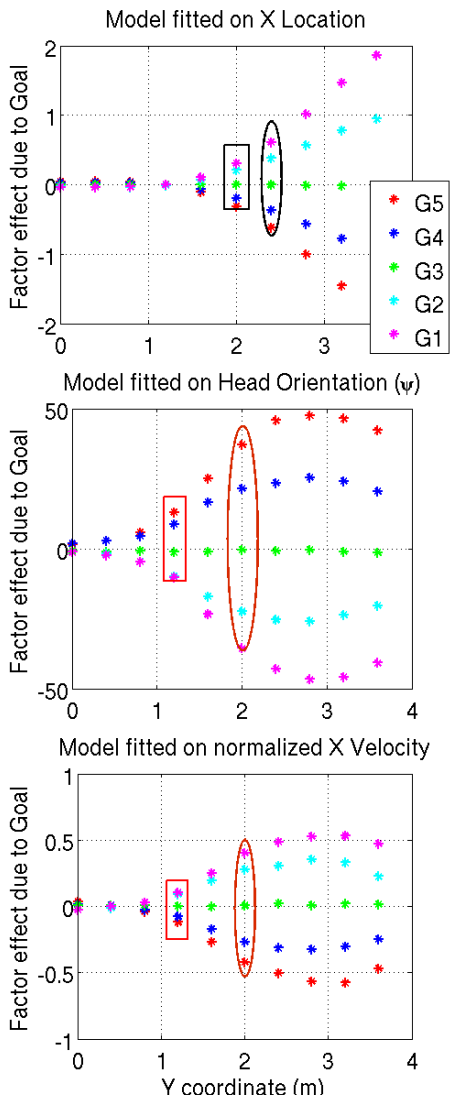

Fig. 4: Estimate of fixed factor effects across all y-locations for x (top), ψ (center) and $\bar{v}_x$ (bottom). The ovals represent the y-location after which Tukey's procedure demonstrated pairwise differences across all pairs with 90% family confidence interval. The rectangles represent the y-location after which differences emerge across the turn directions (i.e., goals G2, G3 and G4).

Fig. 4 depicts a consolidated plot of the fixed factor effects across all y-locations for all three dependent variables: x, $\bar{v}_x$ and ψ. The ovals for each plot represent the y-location after which the fixed factor effects were significant ($p < 0.001$) and Tukey's procedure demonstrated pairwise differences across all pairs with 90% family confidence interval for all subsequent hypotheses of the corresponding variable.

Variation Across Participants: Analysis of the measured data provides strong evidence that a statistically significant difference exists between participants . Interaction effects between the goal location and the participant were also observed. Although this variability is difficult to estimate due to the small sample size, we can still deduce certain characteristics regarding loosely-constrained human motion from the variability observed in the current study.

Anticipatory Turn Signals: Despite the presence of random effects, pairwise comparisons of fixed effects can be used to evaluate the presence of anticipatory turn signals. As mentioned previously, turn signals can be defined as anticipatory if statistically significant differences exist between goal locations for ψ and/or $\bar{v}_x$ at an earlier y-location than that for the dependent variable x, which represents the physical turn. Hence, we examine the pairwise differences estimated using the ANOVA mixed effects model and Tukey's procedure, as summarized in Fig. 4.

The pairwise differences across all pairs emerge for both the turn signals ψ and $\bar{v}_x$ at y-location #6 (indicated by ovals in Fig. 4). In contrast, these pairwise differences are observed across the dependent variable x at y-location #7, which appears later along the path than that for turn signals $\bar{v}_x$ and ψ. Similar, results are obtained when instead of goal locations only the turn directions (left, straight and right) are considered; wherein, the differences for turn signals emerge at y-location #4 (rectangles in Fig. 4), before the differences emerge for the variable x at y-location #6.

Based on the y-location after which the fixed factor effects became significant ($p < 0.001$) and Tukey's procedure demonstrated pairwise differences across all pairs (represented by ovals in Fig. 4), *the data provides evidence of the presence of anticipatory turn signals* for both ψ and $\bar{v}_x$ prior to the physical turn. This is observed despite variation among participants and loosely specified paths. At the current discretization of 0.4 m, the data from our study support the existence of anticipatory turn signals - body velocity and head orientation.

Thus, the results from our study confirm those from prior gait studies reported in [9], [10] that provided evidence for the existence of similar turn signals in purposeful (goal-oriented) human motion. However, statistical tests only provide evidence of the existence of anticipatory indicators; in order to utilize these indicators for path planning, predictive models are required. In the following sections, we explore the utility of these indicators as features in a predictive algorithm in order to investigate their predictive performance.

IV. PREDICTION ALGORITHM

We leverage the prediction algorithm presented in [11], which was designed to predict the goal of human motion from a discrete set of possible targets for which a set of demonstrations have been provided. The method used in [11] was developed in the context of human-robot cooperative manipulation tasks where the set of features was concentrated in the joint angles of the human arms. Here, we take advantage of the possibility of applying this algorithm to a human walking task by using the anticipatory signals, described in the previous section, as features. The anticipatory signals have been identified for turning motion, so additional challenge lies in exploring their utility for predicting arbitrary trajectories. Furthermore, given that this method runs online in real-time, it is ideal for integration in the loop with a motion-planner algorithm.

A. Human Motion Prediction via Anticipatory Signals

The prediction problem is posed in [11] as one of time series classification, which is attempted online using the initial partial segment of the trajectory. The possible motion classes correspond to a statistical model of the demonstrations for each class (each possible target), where each time step t_k is modeled as a multivariate Gaussian with the mean and covariances of the observations of all features f_i as parameters, as illustrated in Fig.5. This model is computed offline to create a library of motions that will be used later to perform the classification.

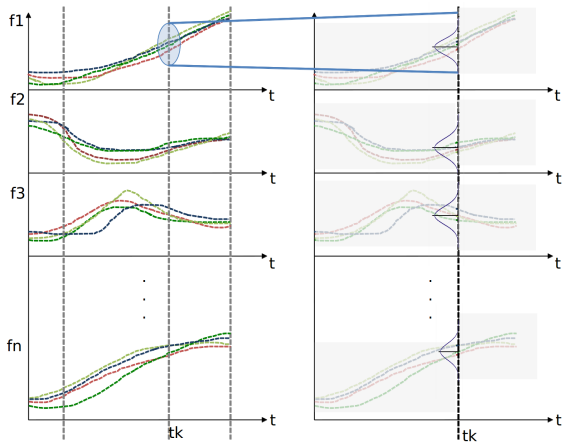

Fig. 5: Multivariate Gaussian model of the time series per time step t_k for one motion class. Each feature f_i has several time series obtained in several demonstrations for one goal.

The online phase computes a classification decision per time step k, selecting the motion class with maximum *a posteriori* probability, computed using the Bayes rule,

$$P(t \mid f_h[1:k]) \propto P(t) \cdot P(f_h[1:k] \mid t), \tag{1}$$

where $P(f_h[1:k] \mid t)$ is the likelihood of observing a particular partial trajectory $f_h[1:k]$ given a motion class t, and $P(t)$ is the prior probability of the motion class t [11]. We use uniform prior for all motion classes. The likelihood term can be computed as shown in Eq.2:

$$P(f_h[1:k] \mid t) = \prod_{k=1}^{K} [\mathcal{N}(\mu_t[k], \Sigma_t[k])]^{\frac{1}{K}}. \tag{2}$$

As proposed in [11], we pre-compute and store in the library terms that are independent of the new performance data, and incorporate dynamic time warping (DTW) [30] to find an optimal alignment for the signals when building the library, as well as incremental online DTW [31] between the motion classes in the library and the test trajectory to be classified. It is interesting to note that, the statistical analysis when performed with the dynamic time wrapped data derived from the original signals, also supports the existence of anticipatory turn signals.

B. Validation of Prediction Using Anticipatory Signals

The performance of the prediction algorithm was assessed through random sub-sampling validation of the data described in SectionIII. The demonstrations were randomly split into a training set and a test set to create a 'random library.' Classification performance is reported per time step as the average correct classification across all test trajectories for all motion classes along all random libraries. This validation process was carried out offline through a simulation of online processing of observed data. For this reason, instead of smoothing the data, the raw position and orientation trajectories were processed through a low-pass filter. Further, the velocities were calculated with a Kalman filter, in which we modeled the motion using a white noise acceleration process model, and used position information as measurements. This signal processing pipeline can be implemented online, as it does not require any future data.

We tested a range of training set sizes to investigate the amount of data required to achieve a certain level of performance. Fig.6b depicts the performance result using the position of the human (x, y) as features, while Fig.6b incorporates head angle (x, y, ψ) and Fig.6c incorporates the velocity of the human $(x, y, \psi, \bar{v}_x, \bar{v}_y)$.

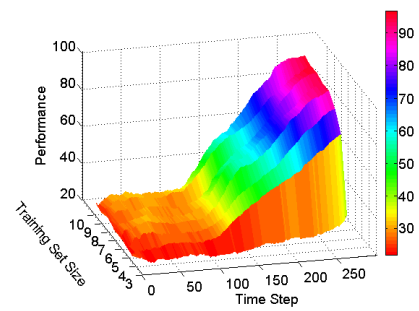

(a) Using (x, y) as features

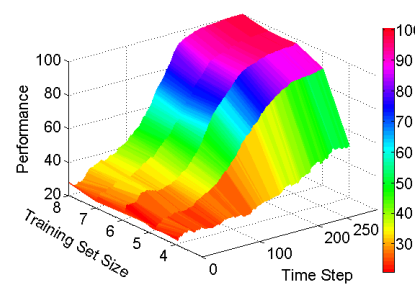

(b) Using (x, y, ψ) as features

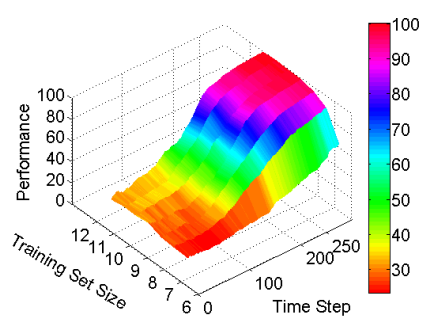

(c) Using $(x, y, \psi, \bar{v}_x, \bar{v}_y)$ as features

Fig. 6: Performance results as a function of time and training set size. Validation using 20 random libraries.

The performance surface obtained when using only position features starts generating prediction results above chance (20% for 5 motion classes) only after the human started to turn in the region of time step 100. In contrast, when incorporating the head orientation, the prediction performance result is in the range 30% to 40% in the second half of the pre-turn region as shown in Fig.6b, giving evidence of the anticipatory power of this feature. For this particular data set, the use of the velocity features didn't achieve better performance than the use of (x, y, ψ) only.

The validation method was also employed in the two different navigation environments considered in Section V. This allowed us to specify the required training set size to achieve the desired predictive performance. The next section discusses the way in which we incorporate this predictive algorithm in a robot planning framework. We note that other methods exist for further augmenting robot planning, including using dynamic models to predict human motion via filtering techniques, such as, Kalman/particle filter or Interacting Multiple Model (IMM) methods [32].

V. USING PREDICTION FOR PLANNING

In the previous section, we evaluated the *predictive* performance of the anticipatory indicators in environments with pre-specified goals. Here, we demonstrate the closed-loop performance of these indicators, using the predictive algorithm in-loop with an anytime path planner designed for dynamic environments. Specifically, we use the anytime, safe-interval path planner (anytime SIPP), a grid-based approach to path planning within dynamic environments [12].

A. Planning Algorithm

The anytime, safe-interval path planner is an extension of grid search-based path planning algorithms that efficiently reasons about predictive information. This is accomplished through the encoding of predictive information in terms of *safe* obstacle-free time intervals, significantly reducing the search space when planning in time. Further, the algorithm assumes the perfect prediction of obstacles over a specified time horizon. We chose this algorithm to demonstrate the closed-loop performance due to its ability to utilize predictive information and reason quickly in time. However, note that the prediction incorporating anticipatory indicators can also be used with other path-planning approaches for dynamic environments, such as those described in Section II.

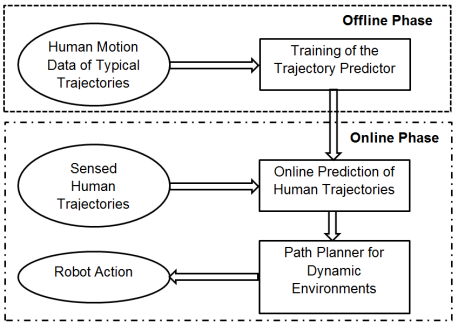

Fig. 7: Schematic of the Prediction and Planning System.

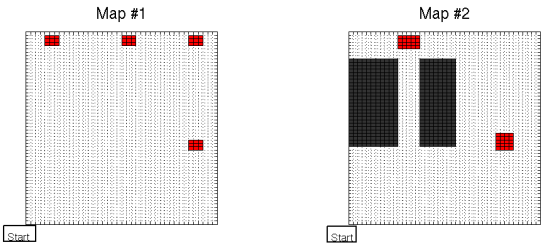

(a) Map 1 (b) Map 2

Fig. 8: The two maps used to demonstrate the integrated co-navigation system. The black squares indicate static obstacles, and the red squares indicate goal locations for human agents. For each run, the human agent begins at the lower left corner and moves toward one of the goal locations. The human motion is simulated using actual human trajectories recorded in a motion capture environment that replicated the above maps.

B. Integrating Prediction and Planning

Figure 7 depicts the framework of the navigation system, which integrates planning and prediction for a given environment. In the offline phase, the prediction algorithm generates the trajectory predictor using human motion data collected from the environment. During the online phase, the algorithm predicts the potential trajectory of a moving human using sensed data such as current position, velocity and orientation. This information is then fed into the planner, which reasons in time and generates time-optimal trajectories for the robot while considering the prospective positions of human agents in the environment. Since the time-step of sensing and prediction is usually smaller than that for the planning algorithm, the prediction algorithm may provide multiple trajectory predictions within a single planning time-step. To account for this, and to ensure safe and collision-free trajectories, we adopted a conservative approach and considered all predicted trajectories as potential obstacles.

C. Simulation Scenario

The aim of the robot is to safely and efficiently navigate within an environment where humans are also moving. The path-planning performance is evaluated with a Matlab simulation, wherein:

- The human trajectories are simulated using data recorded in a motion capture setting,
- The prediction algorithm of Section IV is used to make online predictions about the human agent's prospective path at 100 Hz, and
- The robot replans at 10 Hz using the anytime, safe-interval path planner in order to reach its goal.

For both maps, the motion capture data was collected from the walking motion of one of the experimenters. A total of 20 trials were recorded for each goal location, and 10 trials were used to train and develop the prediction algorithm. Further, in contrast to the study data in SectionIII, the human did not pursue an initial straight line path before turning, but rather pursued unconstrained, goal-oriented motion from the starting location.

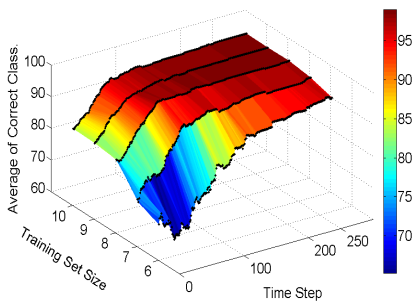

Fig. 9: Prediction performance for Map 2 as a function of time and training set size, with $(x, y, \psi, \bar{v}_x, \bar{v}_y)$ as features.

The prediction algorithm is first trained using motion capture data during the offline phase. Based on the validation, we observed that for both of the environments, better prediction performance is obtained using position, head orientation and normalized velocity as features. Since the human was not asked to follow a specific path at the beginning of the trajectory, the performance of the prediction shown in Fig. 9 achieves a higher initial value from the beginning of the trajectory, equivalent to the post-turn section in Fig. 6c, because this is the point at which the goal-oriented trajectory begins. Through validation, we obtained surface plots as shown in Fig. 9 for each map, and chose a training set of 10 trajectories to generate the predictive model.

The planner assumes that the robot is capable of waiting while generating the plans. Although the planner can handle arbitrary motion, we assume for simplicity that the robot operates with a constant velocity and is capable of only horizontal and vertical motion within the grid world. Further, while considering the humans in the map, the planner extends the obstacle information by 2 grid points in each direction to simulate maintaining a safe and comfortable distance from the human.

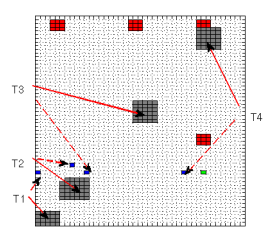

(a) Planning with prediction: Map 1

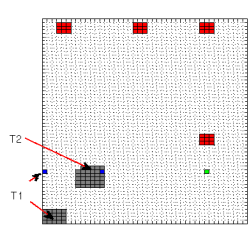

(b) Planning without prediction: Map 1

Fig. 10: Simulation of human-robot co-navigation in Map 1. Without prediction, the robot (shown in blue) collides with the human (grey) at T2; with prediction, the robot allows the human to move first before continuing on to its goal (green).

D. Results

The simulations were carried out with different start and goal locations for the robots, where the human agent chose a particular trajectory in the map. The predictor informed the planner of the future locations of obstacles, and the planner generated a robot trajectory designed to avoid these obstacles. We compared the performance of the co-navigation system with a case for which no predictive information regarding the human agents was available. Here, we describe two such simulation trials, where the effect of prediction and the ability to plan in time is evident. The dynamic simulations are best observed through video footage, included as an attachment and available at http://goo.gl/fOpqx8.

Figures 10-11 provide snapshots of these simulations at different time steps within a single run for each simulation case. The locations of dynamic objects at different time instances are denoted by arrows and colored grid blocks. Namely, the robot is represented with a dashed arrow and blue grid block and the human is represented with a solid arrow and grey grid block. The plots show static obstacles in black, robot goal in green, and possible human goals in red. In both the simulation runs, the human and robot collided when no predictive information was available; this will translate to an extensive waiting time in real-life scenarios due to reactive collision avoidance. However, when predictive information was available, the robot utilized a path that, while of longer length, took less time to complete. This is especially evident in the simulation trial depicted in Fig. 11 where, to avoid a potential conflict while in the corridor, the robot circumnavigated the wall to reach its goal faster.

This proof-of-concept simulation demonstrates the need for prediction in human-robot co-navigation, and supports the usability of the anticipatory indicators and prediction algorithms described in Section III and IV, respectively.

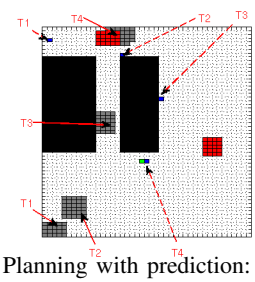

(a) Planning with prediction: Map 2

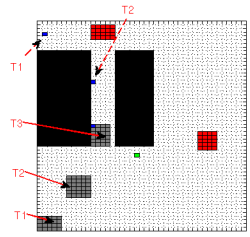

(b) Planning without prediction: Map 2

Fig. 11: Simulation of human-robot co-navigation in Map 2. Without prediction, the robot (show in blue) incorrectly enters the corridor and encounters the human (grey) at T3; with predictive information, the robot chooses a longer path, but eventually reaches its goal (green) faster and without collision.

VI. LIMITATIONS AND FUTURE WORK

In this work, for predicting human motion, we relied on a Vicon motion capture system to track the features to be used by the prediction algorithm. Hence, we required markers to be placed on the human and within a structured environment. Future work will include an exploration of the prediction capability of the algorithm while using on-board, markerless sensors, and how the uncertainty will propagate to the predictor through the closed loop. Also, in this work, the co-navigation system was tested using Matlab simulation. We aim to implement the system online using Robot Operating System for testing on robot hardware. A hardware implementation of this system will require other safety considerations, including recovery behaviors for when the robot incorrectly predicts motion trajectories, or when humans change their paths/intention midway through their motion.

Additionally, the planning and prediction system described above did not take into consideration any modifications to the human path as a result of the motion of the robot. Prior work [7] has demonstrated the importance of this interactive behavior for path planning within crowded environments. Further, a robot can also communicate its intention (such as its prospective path), which can in turn impact the motion of human agents. In the future, we intend to leverage this interactive behavior and communication by developing planning strategies that can reason over both human and robot agents simultaneously.

VII. CONCLUSION

Mobile, interactive robots that function in close proximity with humans require the ability to *predict* and *plan* around uncertain, dynamic human agents within their surroundings. Path prediction can be improved through the consideration of biomechanical aspects of human motion. Through a biomechanical study, we confirmed the existence of anticipatory turn indicators for human walking motion. The efficacy of these indicators was demonstrated using a target prediction algorithm to predict human motion in environments with predefined goals. Lastly, the effect of this predictive capability for planning paths was evaluated in simulation using anytime safe-interval path planning, and significant benefits were observed. Future directions for this work include evaluation of the system within an uncontrolled, physical scenario requiring human-robot interaction.

REFERENCES

[1] S. M. LaValle, *Planning algorithms*. Cambridge university press, 2006.

[2] S. M. LaValle, "Motion planning for dynamic environments," in *ICRA*, 2012.

[3] G. Hoffman and C. Breazeal, "Effects of anticipatory action on human-robot teamwork efficiency, fluency, and perception of team," in *HRI*, 2007.

[4] F. Large, D. Vasquez, T. Fraichard, and C. Laugier, "Avoiding cars and pedestrians using velocity obstacles and motion prediction," in *Intelligent Vehicles Symposium*, 2004.

[5] B. D. Ziebart, N. Ratliff, G. Gallagher, C. Mertz, K. Peterson, J. A. Bagnell, M. Hebert, A. K. Dey, and S. Srinivasa, "Planning-based prediction for pedestrians," in *IROS*, 2009.

[6] M. Kuderer, H. Kretzschmar, C. Sprunk, and W. Burgard, "Feature-based prediction of trajectories for socially compliant navigation," in *R:SS*, 2012.

[7] P. Trautman, J. Ma, R. M. Murray, and A. Krause, "Robot navigation in dense human crowds: the case for cooperation," in *ICRA*, 2013.

[8] T. Bandyopadhyay, K. S. Won, E. Frazzoli, D. Hsu, W. S. Lee, and D. Rus, "Intention-aware motion planning," in *WAFR*, 2013.

[9] A. E. Patla, A. Adkin, and T. Ballard, "Online steering: coordination and control of body center of mass, head and body reorientation," *Experimental Brain Research*, vol. 129, no. 4, pp. 629–634, 1999.

[10] L. Stirling and J. Weatherly, "Examining anticipatory turn signaling in typically developing 4-and 5-year-old children for applications in active orthotic devices," *Gait & Posture*, vol. 37, no. 3, 2013.

[11] C. Pérez-D'Arpino and J. Shah, "Fast target prediction of human reaching motion for cooperative human-robot manipulation tasks using time series classification," in *ICRA*, 2015.

[12] V. Narayanan, M. Phillips, and M. Likhachev, "Anytime safe interval path planning for dynamic environments," in *IROS*, 2012.

[13] D. Ferguson and A. Stentz, "Anytime RRTs," in *IROS*, 2006.

[14] M. Likhachev, D. Ferguson, G. Gordon, A. Stentz, and S. Thrun, "Anytime search in dynamic graphs," *Artificial Intelligence*, vol. 172, no. 14, pp. 1613–1643, 2008.

[15] C. Fulgenzi, C. Tay, A. Spalanzani, and C. Laugier, "Probabilistic navigation in dynamic environment using rapidly-exploring random trees and gaussian processes," in *IROS*, 2008.

[16] G. S. Aoude, B. D. Luders, J. M. Joseph, N. Roy, and J. P. How, "Probabilistically safe motion planning to avoid dynamic obstacles with uncertain motion patterns," *Autonomous Robots*, vol. 35, no. 1, pp. 51–76, 2013.

[17] T. Kruse, A. K. Pandey, R. Alami, and A. Kirsch, "Human-aware robot navigation: A survey," *Robotics and Autonomous Systems*, vol. 61, no. 12, pp. 1726–1743, 2013.

[18] J. C. Boerkoel Jr and J. A. Shah, "Planning for flexible human-robot co-navigation in dynamic manufacturing environments," in *HRI Pioneers*, 2013.

[19] E. A. Sisbot, L. F. Marin-Urias, R. Alami, and T. Simeon, "A human aware mobile robot motion planner," *IEEE Transactions on Robotics*, vol. 23, no. 5, pp. 874–883, 2007.

[20] C. Dondrup, C. Lichtenthäler, and M. Hanheide, "Hesitation signals in human-robot head-on encounters: a pilot study," in *HRI*, 2014.

[21] T. Kruse, P. Basili, S. Glasauer, and A. Kirsch, "Legible robot navigation in the proximity of moving humans," in *IEEE Workshop on Advanced Robotics and its Social Impacts (ARSO)*, 2012.

[22] A. Dragan and S. Srinivasa, "Generating legible motion," in *R:SS*, 2013.

[23] M. Zhao, R. Shome, I. Yochelson, K. E. Bekris, and E. Kowler, "An experimental study for identifying features of legible manipulator paths," in *Intl. Symposium on Experimental Robotics (ISER)*, 2014.

[24] M. Bennewitz, W. Burgard, G. Cielniak, and S. Thrun, "Learning motion patterns of people for compliant robot motion," *IJRR*, vol. 24, no. 1, pp. 31–48, 2005.

[25] D. Helbing and P. Molnar, "Social force model for pedestrian dynamics," *Physical review E*, vol. 51, no. 5, p. 4282, 1995.

[26] P. Henry, C. Vollmer, B. Ferris, and D. Fox, "Learning to navigate through crowded environments," in *ICRA*, 2010.

[27] J. Joseph, F. Doshi-Velez, A. S. Huang, and N. Roy, "A bayesian nonparametric approach to modeling motion patterns," *Autonomous Robots*, vol. 31, no. 4, pp. 383–400, 2011.

[28] G. Aoude, J. Joseph, N. Roy, and J. How, "Mobile agent trajectory prediction using bayesian nonparametric reachability trees," in *AIAA Infotech@ Aerospace*, 2011.

[29] R. Jategaonkar, *Flight vehicle system identification: a time domain methodology*. AIAA, 2006.

[30] J. Kruskall and L. M, "The symmetric time warping problem from continuous to discrete," in *Time Warps String Edits and Macromolecules: The Theory and Practice of Sequence Comparison*, (Addison-Wesley Publishing Co.), pp. 125 – 161, 1983.

[31] S. Dixon, "Live tracking of musical performances using on-line timewarping," in *Intl. Conf. on Digital Audio Effects*, 2005.

[32] Y. Bar-Shalom, X. R. Li, and T. Kirubarajan, *Estimation with applications to tracking and navigation: theory algorithms and software*. John Wiley & Sons, 2004.